J Fluoresc (2010) 20:329–342
DOI 10.1007/s10895-009-0561-0

ORIGINAL PAPER

Rare Earth Complexes with 3-Carbaldehyde Chromone-(Benzoyl) Hydrazone: Synthesis, Characterization, DNA Binding Studies and Antioxidant Activity

Yong Li · Zheng-yin Yang

Received: 31 May 2009 / Accepted: 12 October 2009 / Published online: 24 October 2009

Abstract A new ligand, 3-carbaldehyde chromone-(benzoyl) hydrazone (L), was prepared by condensation of 3-carbaldehyde chromone with benzoyl hydrazine. Its four rare earth complexes have been prepared and characterized on the basis of elemental analyses, molar conductivities, mass spectra, ^{1}H NMR spectra, UV-vis spectra, fluorescence studies and IR spectra. The Sm(III) complex exhibits red fluorescence under UV light and the fluorescent properties of Sm(III) complex in solid state and different solutions were investigated. In addition, the DNA binding properties of the ligand and its complexes have been investigated by electronic absorption spectroscopy, fluorescence spectra, ethidium bromide displacement experiments, iodide quenching experiments, salt effect and viscosity measurements. Experimental results suggest that all the compounds can bind to DNA via an intercalation binding mode. Furthermore, the antioxidant activities of the ligand and its complexes were determined by superoxide and hydroxyl radical scavenging methods in vitro. The rare earth complexes were found to possess potent antioxidant activities that are better than those of the ligand alone.

Keywords 3-carbaldehyde chromone-(benzoyl) hydrazone · Rare earth complexes · Fluorescence spectra · DNA binding properties · Antioxidant activity

Y. Li · Z.-y. Yang (✉)
College of Chemistry and Chemical Engineering and State Key Laboratory of Applied Organic Chemistry, Lanzhou University, Lanzhou 730000, People's Republic of China
e-mail: yangzy@lzu.edu.cn

Introduction

DNA plays an important role in the life process since it contains all the genetic information for the cellular function. However, DNA molecules are prone to be damaged under various conditions such as interactions with some small molecules. This damage may lead to various pathological changes in living organisms. The interaction of metal complexes with DNA is of great interest in design and development of synthetic restriction enzymes, chemotherapeutic drugs and DNA foot printing agents [1–4]. Metal complexes can bind to DNA in non-covalent ways such as electrostatic effect, groove binding and intercalation. However, considerable useful applications of the metal complexes require that the complexes can bind to DNA via an intercalation mode which could induce cellular degradation [5]. It was reported the ability of metal complexes intercalating into DNA will increase with the planarity of the ligand [6, 7]. The coordination geometry and ligand donor atom type also play key roles in determining the binding extent of complexes to DNA [8, 9]. Additionly, both the metal ion type and its valence also play important roles in deciding extent of complexes to DNA [10]. Among all the metal complexes, rare earth complexes are widely investigated since the rare earth complexes with tetracycline, phenanthroline [11], adriamycin and pyridine [12–14] have been synthesized as a probe to study nucleic acids.

Chromones (1-benzopyran-4-one) are a group of naturally and widely distributed compounds that are ubiquitous in nature, especially in the plant kingdom [15]. These compounds have attracted a great deal of attention and many synthesized chromone derivatives have been widely studied due to their biological activities including antimycobacterial, antifungal, anticonvulsant, antimicrobial and mushroom tyrosinase inhibition activities [16, 17]. These

derivatives also serve as intermediates to many products of fine chemical industries such as pharmaceuticals, agrochemicals and dyestuffs [18]. In this regard, as a further research, a new Schiff-base ligand, 3-carbaldehyde chromone-(benzoyl) hydrazone (L) and its rare earth complexes were synthesized and their DNA binding properties were investigated systematically. In addition, the antioxidant activities of the ligand and its complexes were determined by superoxide and hydroxyl radical scavenging methods in vitro. Furthermore, the Sm(III) complex can emit intrinsic spectra under excitation both in solid state and organic solvents, which may provide more advantages to be applied as a candidate of anticancer drugs and nucleic acid probe.

Experimental section

Materials and instrumentation

Ethidium bromide (EB) and calf thymus DNA (CT DNA) were purchased from Sigma Chemical Co.. All chemicals and solvents used were of analytical reagent grade and used without further purification unless otherwise noted.

All the experiments involved with the interaction of the ligand and complexes with CT DNA were carried out in doubly distilled water buffer containing 5 mM Tris [Tris (hydroxymethyl)-aminomethane] and 50 mM NaCl and adjusted to pH 7.1 with hydrochloric acid. Solution of CT DNA in the buffer gave ratios of UV absorbance of about 1.8–1.9:1 at 260 and 280 nm, indicating that the CT DNA was sufficiently free of protein [19]. The CT DNA concentration per nucleotide was determined spectrophotometrically by employing an extinction coefficient of 6,600 M^{-1} cm^{-1} at 260 nm [20]. The ligand and complexes were dissolved in a solvent mixture of 1% DMF and 99% Tris-HCl buffer (pH 7.1) at the concentration 1.0×10^{-5} M.

Carbon, hydrogen and nitrogen were determined using an Elemental Vario EL analyzer. The metal contents of the complexes were determined by titration with EDTA (xylenol orange tetrasodium salt used as an indicator and hexamethylidynetetraimine as buffer). The melting point of the ligand was determined on a Beijing XT4-100X microscopic melting point apparatus (the thermometer was not corrected). The IR spectra were obtained in KBr discs on a Therrno Mattson FTIR spectrophotometer in the 4,000 −400 cm^{-1} region. ^{1}H NMR spectra were recorded on a Varian VR 300 MHz spectrometer in DMSO-d^6 with TMS (tetramethylsilane) as an internal standard. Mass spectra were performed on a APEX II FT-ICR MS instrument using DMF as mobile phase. Conductivity measurements were performed in DMF solution with a DDS-11C conductometer at 25.0 °C. The UV-vis spectra were recorded on a Shimadzu UV-240 spectrophotometer. Fluorescence spectra were recorded on a Hitachi RF-4500 spectrofluorophotometer at a constant room temperature. Its measuring wavelength range (on both EX and EM) is from 200 to 730 nm, and the spectral resolution is 1.0 nm. In addition, its light source and detector are 150 W xenon lamp and R3788 photomultiplier tube, respectively. Quantum yields of the ligand and its complexes were determined by an absolute method using an integrating sphere on FLS-920 of Edinburgh instrument with coumarin 307 as the reference sample. The FLS-920 is equipped by a pulsed xenon lamp as the excitation source, a raster as the detector and with spectral resolution of 0.05 nm.

DNA binding studies

Electronic absorption spectroscopy

Electronic absorption titration experiments were performed with fixed concentration drugs (10 μM), while gradually increasing the concentration of CT DNA. When measuring the absorption spectra, an equal amount of CT DNA was added to both the complex solutions and the reference solution to eliminate the absorbance of CT DNA itself. Each sample solution was scanned in the range of 190–500 nm.

Fluorescence spectra

Fixed amounts (10 μM) of compounds were titrated with increasing amounts of CT DNA, over a range of DNA concentrations from 2.5 to 15 μM. Excitation wavelengths of the samples were about 345 nm, scan speed was 480 nm/min, slit width was 5 nm. All experiments were conducted at a constant room temperature in a buffer solution containing 5 mM Tris-HCl (pH 7.1) and 50 mM NaCl concentrations. The intrinsic binding constants (K_b) of the compounds with DNA were obtained through fluorescence spectra according to the following equation [21]:

$$r/C_f = K_b \times (n - r)$$

$$C_b = C_t\left[\left(F - F^0\right)/\left(F^{max} - F^0\right)\right],$$

where C_t is the total compound concentration, F is the observed fluorescence emission intensity at given DNA concentrations, F^0 is the intensity in the absence of DNA and F^{max} is the fluorescence of the totally bound compound. Binding data were cast into the form of a Scatchard plot of r/C_f versus r, where r is the binding ratio $C_b/[DNA]_t$, C_f is the free compound concentration and n is the binding site number.

Further support for the mode of the ligand and complexes binding to DNA is given through the emission quenching experiments. A 2.0 mL solution of 4 μM DNA

and 0.32 μM EB (at saturating binding levels) was titrated by 2.5–50 μM the complexes and ligand at a constant room temperature in a buffer solution containing 5 mM Tris-HCl (pH 7.1) and 50 mM NaCl concentrations. Quenching data were analyzed according to the Stern-Volmer equation which could be used to determine the fluorescent quenching mechanism:

$$F_o/F = 1 + K_q[Q],$$

Where F_o and F are the fluorescence intensity in the absence and presence of drug at [Q] concentration respectively; K_q is the quenching constant and [Q] is the quencher concentration. Plots of F_o /F versus [Q] appear to be linear and K_q depends on temperature [22].

Iodide quenching experiments were done according to the below methods: fluorescence intensities were recorded in the absence and presence of DNA in the mixture solution of each compound and KI. The fluorescence quenching efficiency is evaluated by Stern-Volmer K_{sv}, which varies with the experimental conditions. Quenching plots were constructed according to the following Stern-Volmer equation.

$$F_o/F = 1 + K_{sv}[I^-],$$

Where F_o and F are the fluorescence intensity in the absence and presence of iodide at [I^-] concentration, respectively; K_{sv} is the quenching constant and [I^-] is the concentration of iodide. Plots of F_o /F versus [I^-] appear to be linear and K_{sv} was evaluated by linear least-squares analysis of the data according to the equation [23].

Fluorescence intensities were also recorded in the absence and presence of DNA in the mixture solution of each compound and NaCl to investigate the salt effects of compounds to DNA.

Viscosity measurements

Viscosity experiments were conducted on an Ubbelodhe viscometer, immersed in a thermostated water-bath maintained to 25.0±0.1 °C. Titrations were performed for the complexes (0.5–4 μM), and each compound was introduced into a DNA solution (5 μM) present in the viscometer. Data were presented as $(\eta/\eta_0)^{1/3}$ versus the ratio of the concentration of the compound and DNA, where η is the viscosity of DNA in the presence of the compound and η_0 is the viscosity of DNA alone [24, 25].

Antioxidant activity

In antioxidant activity experiments the superoxide radicals ($O_2^{\bullet-}$) were produced by the system MET/$VitB_2$/NBT [26]. The amount of $O_2^{\bullet-}$ and suppression ratio for $O_2^{\bullet-}$ can be calculated by measuring the absorbance at 560 nm, because NBT can be reduced quantitatively to blue formazan by $O_2^{\bullet-}$. The solution of MET, $VitB_2$ and NBT were prepared with 0.067 M phosphate buffer (pH=7.8) at the condition of avoiding light. The tested compounds were dissolved in DMF. The reaction mixture contained MET (0.01 mol L^{-1}), NBT (4.6×10^{-5} mol L^{-1}), $VitB_2$ (3.3×10^{-6} mol L^{-1}), phosphate buffer solution (0.067 mol L^{-1}) and the tested compound (the final concentration: $C_{i\ (i=1-6)}$=0.4, 1.0, 2.0, 4.0, 6.0, 8.0 μM). After incubating at 30 °C for 10 min and illuminating with a fluorescent lamp for 3 min, the absorbance (A_i) of the samples were measured at 560 nm. The sample without the tested compound and avoiding light was used as the control. The suppression ratio for $O_2^{\bullet-}$ was calculated from the following expression:

$$\text{Suppression ratio}\ (\%) = [(A_0 - A_i)/A_0] \times 100\%$$

where A_i = the absorbance in the presence of the ligand or its complexes, A_0 = the absorbance in the absence of the ligand or its complexes.

In antioxidant activity experiments the hydroxyl radical ($HO^{\bullet}$) in aqueous media was generated through the Fenton reaction [27]. The solution of the tested compounds was prepared with DMF. The reaction mixture contained 2.5 mL 0.15 M phosphate buffer (pH=7.4), 0.5 mL 114 μM safranin, 1 mL 945 μM EDTA-Fe(II), 1 mL 3% H_2O_2 and 30 μL the tested compound solution (the final concentration: $C_{i\ (i=1-6)}$=1.0, 2.0, 3.0, 4.0, 5.0, 6.0 μM). The sample without the tested compound was used as the control. The reaction mixtures were incubated at 37 °C for 60 min in a water-bath. Absorbances (A_i, A_0, A_c) at 520 nm were measured. The suppression ratio for $HO^{\cdot}$ was calculated from the following expression:

$$\text{Suppression ratio}\ (\%) = [(A_i - A_0)/(A_c - A_0)] \times 100\%$$

Where A_i = the absorbance in the presence of the tested compound; A_0 = the bsorbance in the absence of the tested compound; A_c = the absorbance in the absence of the tested compound, EDTA-Fe(II) and H_2O_2.

The antioxidant activity was expressed as the 50% inhibitory concentration (IC_{50}). IC_{50} values were calculated from regression lines where: x was the tested compound concentration in mM and y was percent inhibition of the tested compounds.

Preparation of the ligand (L)

Scheme of the synthesis of the ligand is shown in Fig. 1. 3-carbaldehyde chromone was prepared according to the literature methods [28]. An ethanol solution containing benzoyl hydrazine (1.36 g, 10 mmol) was added dropwise

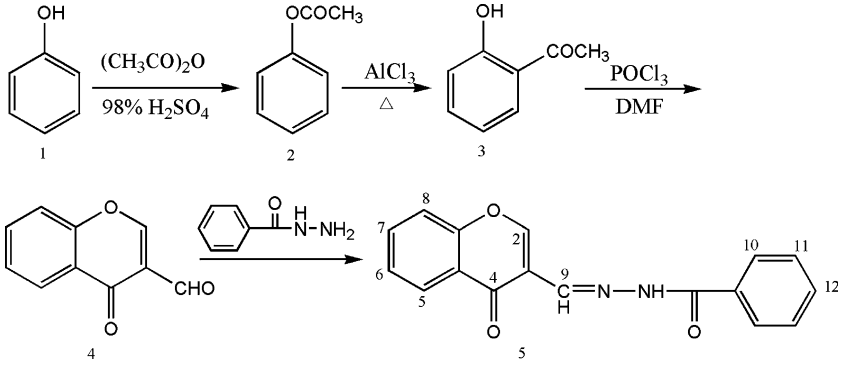

Fig. 1 Scheme of the synthesis of the ligand (L)

to another ethanol solution containing 3-carbaldehyde chromone (1.74 g, 10 mmol). The mixture was refluxed on an oil bath for 4 h with stirring and a yellow precipitate formed. The yellow precipitate was filtered, washed several times with ethanol and recrystallized from DMF and water to give the ligand (L), which was dried in a vacuum. Yield: 82.16%. Mp 176–178 °C. Anal. Calcd for $C_{17}H_{12}N_2O_3$: C, 69.86; H, 4.14; N, 9.58. Found: C, 69.92; H, 4.174; N, 9.49. IR ν_{max} (cm^{-1}): $\nu_{(carbonyl)C=O}$: 1,679, $\nu_{(hydrazonic)C=O}$: 1,639, $\nu_{C=N}$: 1,600 cm^{-1}. U_{max} (nm): 273, 303 nm.

Preparation of the complexes

The ligand (1.0 mmol, 0.292 g) and the La(III) nitrate (1.0 mmol, 0.434 g) were added together in ethanol (20 mL). The mixture solution was refluxed on an oil bath for 2 h with stirring and a white precipitate, the La(III) complex, was separated from the solution by suction filtration, purified by washing several times with ethanol and dried for 24 h in a vacuum. Sm(III), Nd(III) and Tb(III) complexes were prepared by the same way. Anal. Calcd for La(III) complex $C_{34}H_{24}N_7O_{15}La$: C, 44.90; H, 2.66; N, 10.78; La, 15.27. Found: C, 44.82; H, 2.61; N, 10.75; La, 15.30. IR ν_{max} (cm^{-1}): $\nu_{(carbonyl)C=O}$: 1,643, $\nu_{(hydrazonic)C=O}$: 1,620, $\nu_{C=N}$: 1,569, ν_{NO_3}: 1,482, 1,385, 1,327, 1,185, 819, ν_{M-O}: 605, ν_{M-N}: 418 cm^{-1}. U_{max} (nm): 277, 308 nm. Λ_m (S cm^2 mol^{-1}): 117. Anal. Calcd for Sm(III) complex $C_{34}H_{24}N_7O_{15}Sm$: C, 44.34; H, 2.63; N, 10.65; Sm, 16.33. Found: C, 44.52; H, 2.69; N, 10.54; Sm, 16.38. IR ν_{max} (cm^{-1}): $\nu_{(carbonyl)C=O}$: 1,642, $\nu_{(hydrazonic)C=O}$: 1,618, $\nu_{C=N}$: 1,574, ν_{NO_3}: 1,481, 1,384, 1,322, 1,185, 817, ν_{M-O}: 610, ν_{M-N}: 421 cm^{-1}. U_{max} (nm): 277, 307 nm. Λ_m (S cm^2 mol^{-1}): 100. Anal. Calcd for Nd(III) complex $C_{34}H_{24}N_7O_{15}Nd$: C, 44.64; H, 2.64; N, 10.72; Nd, 15.77. Found: C, 44.62; H, 2.71; N, 10.77; Nd, 15.65. IR ν_{max} (cm^{-1}): $\nu_{(carbonyl)C=O}$: 1,639, $\nu_{(hydrazonic)C=O}$: 1,618, $\nu_{C=N}$: 1,574, ν_{NO_3}: 1,483, 1,382, 1,320, 1,187, 818, ν_{M-O}: 609, ν_{M-N}: 420 cm^{-1}. U_{max} (nm): 277, 308 nm. Λ_m (S cm^2 mol^{-1}): 99. Anal. Calcd for Tb(III) complex $C_{34}H_{24}N_7O_{15}NTb$: C, 43.93; H, 2.60; N, 10.55; Tb, 17.10. Found: C, 43.82; H, 2.73; N, 10.67; Tb, 17.15. IR ν_{max} (cm^{-1}): $\nu_{(carbonyl)C=O}$: 1,639, $\nu_{(hydrazonic)C=O}$: 1,614, $\nu_{C=N}$: 1,563, ν_{NO_3}: 1,489, 1,384, 1,317, 1,194, 822, ν_{M-O}: 639, ν_{M-N}: 429 cm^{-1}. U_{max} (nm): 276, 307 nm. Λ_m (S cm^2 mol^{-1}): 102.

Results and discussion

The complexes were prepared by direct reaction of the ligand with appropriate mole ratios of Ln(III) nitrate in ethanol. The yields were good to moderate. The complexes are stable in atmospheric conditions for extended periods and easily soluble in DMF and DMSO; slightly soluble in ethanol, methanol and acetone; insoluble in benzene, water and diethyl ether. The molar conductivities of the complexes are around 99 – 117 in DMF solution and in accord with them being formulated as 1:1 electrolytes [29]. The structures of the complexes were characterized on the basis of elemental analyses, molar conductivities, mass spectra, ^{1}H NMR spectra, UV-vis spectra, fluorescence studies and IR spectra. The elemental analyses and molar conductivities show that formulas of the complexes conform to [Ln L_2•$(NO_3)_2$]•NO_3 [Ln(III) = La, Sm, Nd and Tb; L is the ligand 3-carbaldehyde chromone-(benzoyl) hydrazone].

Structure of the complexes

IR spectra

The IR spectra of the complexes are similar and IR spectra usually provide a lot of valuable information on coordination reaction. All the spectra are characterized by vibrational bands mainly due to the C = O, C = N and NO_3 groups. The $\nu_{(carbonyl)C=O}$ and $\nu_{(hydrazonic)C=O}$ vibrations of the free ligand appear at 1,679 and 1,639 cm^{-1}, respectively; for the complexes these peaks shift to 1,642 and 1,618 cm^{-1} or so, $\Delta\nu_{(ligand\text{-}complexes)}$ is equal to 37 and 21 cm^{-1}. In the complexes, the band at 610 cm^{-1} or so is assigned to ν_{M-O}. It demonstrates that the oxygen of

carbonyl has formed a coordinative bond with the rare earth ions [30]. The different shifts of the wavenumbers indicate that the Ln-O (carbonyl) bond is stronger than the Ln-O (hydrazonic) bond. The band at 1,600 cm^{-1} for the free ligand is assigned to the $\nu_{C=N}$ stretch, which shifts to about 1,574 cm^{-1} for the complexes, $\Delta\nu_{(ligand\text{-}complexes)}$ is equal to 26 cm^{-1}. Weak bands at 420 cm^{-1} or so are assigned to $\nu_{M\text{-}N}$ in the complexes. These shifts and new bands further confirm that the nitrogen of the imino-group bonds to the rare earth ions [31]. The absorption bands of the coordinated nitrates were observed at about 1,481 (ν_{as}) and 820 (ν_s) cm^{-1}. The ν_3 (E') free nitrates appear at 1,384 cm^{-1} in the spectra of the rare earth complexes. In addition, the separation of the two highest frequency bands $|\nu_4 - \nu_1|$ is approximately 165 cm^{-1}, and accordingly the coordinated NO_3^- anion in the complexes is a bidentate ligand [32].

UV-vis spectra

The study of the electronic spectra in the ultraviolet and visible (UV-vis) ranges for the rare earth complexes and ligand was carried out in a buffer solution containing 5 mM Tris-HCl (pH 7.1) and 50 mM NaCl concentrations. The electronic spectra of the free ligand have a strong band at U_{max}=273 nm and a medium band at U_{max}=303 nm. The complexes also yield two bands and the two bands are shifted to 277 and 308 nm or so. These indicate that the rare earth complexes are formed.

Mass spectra

The electrospray ionization (ESI) mass spectra of La (III) complex were made. The mass spectra of La (III) complex show peaks at 847, 784, and 721 which can be assigned to the fragments $[La(III)\ complex–NO_3]^+$, $[La(III)\ complex–2NO_3–H]^+$ and $[La(III)\ complex–3NO_3–2H]^+$, respectively.

^1H NMR spectra

The ^1H NMR spectra of the ligand and its La (III) complex are assigned as follows: L (DMSO-d^6 300 MHz): δ 11.96 (1H, s, = NNH, exchangeable with D_2O), 8.85 (1H, s, 2-H), 8.65 (1H, s, 9-H), 8.15 (1H, dd, J=1.2, 8.1 Hz, 7-H), 8.14-7.85 (3H, m, PhH, 5, 8, 12-H), 7.75 (1H, dd, J=1.2, 8.1 Hz, 6-H), 7.57-7.53 (4H, m, PhH, 10, 11-H). $[La\ L_2\bullet(NO_3)_2]\bullet NO_3$ (DMSO-d^6 300 MHz): δ 11.91 (2H, s, = NNH), 8.84 (2H, s, 2-H), 8.63 (2H, s, 9-H), 8.11 (2H, dd, J=0.8, 7.2 Hz, 7-H), 8.06-7.90 (6H, m, PhH, 5, 8, 12-H), 7.83 (2H, dd, J=0.8, 7.2 Hz, 6-H), 7.71-7.59 (8H, m, PhH, 10, 11-H). The hydrogen of the = NNH- group is still detected in the complexes and there were no hydrogens displaced by metal, which is also supported by the above investigations.

Fluorescence studies

The emission spectra of the ligand and Sm(III) complex in solid state (both the excitation and emission slit widths were 1.5 nm) were recorded at room temperature. The Sm(III) complex exhibits red fluorescence and the emission is readily observed with naked eyes under UV light, whereas, the fluorescence intensities of other rare earth complexes are much too weak in the solid state, which are not discussed in our present work. Fluorescence spectra of the ligand and Sm(III) complex in solid state are shown in Fig. 2. Based on the theory of antenna effect [33, 34], the intensity of luminescence of Ln(III) complexes is related to the efficiency of the intramolecular energy transfer between the triple level of the ligand and the emitting level of the metal ions, which depends on the energy gap between the two levels. In the solid state, probably the energy gap between the ligand's triplet levels and the emitting levels of the Sm(III) favors the energy transfer process for samarium, which makes Sm(III) complex show the most intense red fluorescence. However, other rare earth complexes do not exhibit fluorescence, indicating that energy transfer process between the ligand's triplet levels and the emitting levels of other rare earth ions is not favored. Furthermore, the excitation and emission spectra of the rare earth complexes were obtained and their relative fluorescence intensities are very low comparing with the Sm (III) complex under the same conditions (the excitation and emission slit widths are both 1.5 nm). The excitation and emission wavelengths are 343, 421 nm (La(III) complex), 344, 559 nm (Sm(III) complex), 393, 489 nm (Nd(III) complex) and 390, 482 nm (Tb(III) complex), respectively. Because La(III) ion has no 4f electrons and La(III) complex shows no characteristic fluorescence, it is not necessary to discuss its luminescent properties. In order to clarify the

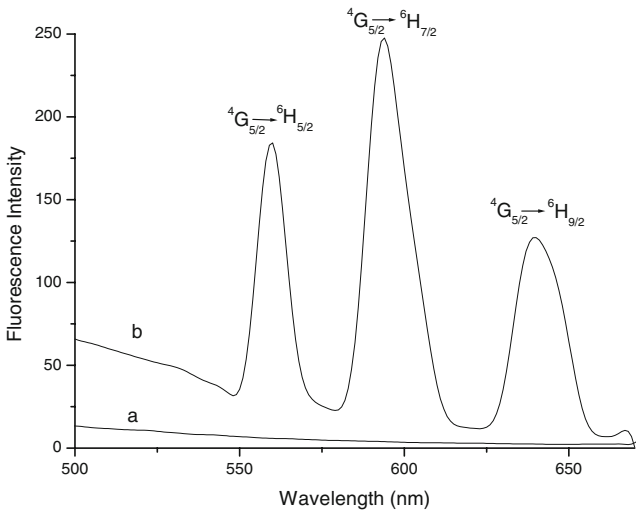

Fig. 2 Solid state emission spectra of the ligand **a** (λ_{ex}=343 nm, λ_{em}=449 nm) and Sm(III) complex **b** (λ_{ex}=344 nm, λ_{em}=559 nm)

ligand's triplet level, a new coordination compound, [Gd L_2•$(NO_3)_2$]•NO_3 was prepared according to the previous method and its phosphorescence spectrum was measured at 77K in DMF solution (1×10^{-5} mol/L). The lowest triplet-state level energy (T) of the ligand was calculated by the shortest wavelength transition in the phosphorescence spectrum to be 21,008 cm^{-1} (476 nm) [35]. This energy level is above the resonance level $^4G_{5/2}$ of Sm(III), $^5D_4$ of Tb(III) and $^4F_{3/2}$ of Nd(III) ions. Thus the absorbed energy could be transferred from the ligand to Sm(III), Tb(III) or Nd(III) ion. However, the intramolecular transfer efficiency depends chiefly on two energy transfer processes: one is from the lowest triplet level (T) of ligand to the resonance level of Sm(III) ion ($^4G_{5/2}$) by resonant exchange interaction, and the other is just an inverse energy transfer by the thermal de-excitation mechanism [36, 37]. Established on this theory, the conclusion can be drawn that energy gap between T and $^4G_{5/2}$ is of opposite influence on the two energy transfer processes and an optimal value can be assumed to exist. In addition, based on the view of numerical point, the strong fluorescence of the Sm(III) complex is due to the optimal ($\Delta\nu$=3,119 cm^{-1}), and it should be better than that of Tb(III) complex ($\Delta\nu$=261 cm^{-1}) and Nd(III) complex ($\Delta\nu$=558 cm^{-1}) [38]. Too large or small energy gap affects the energy transfer from the ligand and rare earth ions and then the fluorescence of the complexes would be quenched. That is why Sm(III) complex can emit characteristic fluorescence, whereas other investigated rare earth complexes can not exhibit their characteristic luminescence [39].

The influence of solvents on the fluorescence intensities of the ligand and Sm(III) complex was also investigated. As shown in Table 1, the fluorescence intensities of Sm(III) complex in organic solvents are obviously weaker than that of the powder. This may be due to the quenching process of solvent molecules in the solution. The energy transfer from the triplet excited state of the ligand to the emitting level of the samarium ion could not be carried out perfectly because the oscillatory motions of the entering solvent molecules may consume more energy. All these indicate that the polarity of the solvents affects the fluorescence of Sm(III) complex. In addition, the detailed differences in the optical measurement conditions also affect the influence of solvents. The solid emission spectrum of the Sm(III) complex was determined on a Hitachi RF-4500 spectrofluorophotometer, whereas its emission spectra and quantum yields in different organic solvents were determined on FLS-920 of Edinburgh instrument. The two instruments have different detectors, resolutions and so on, so the different instruments also exert certain influence on the fluorescence intensities. Furthermore, the fluorescence quantum yields of Sm(III) complex are significantly higher than the free ligand, indicating that Sm(III) complex will be a good candidate for biological use and red emitter in electroluminescence devices.

Since the crystal structures of the rare earth complexes have not been obtained yet, we characterized the complexes and determined its possible structure by elemental analyses, molar conductivities, IR spectra, mass spectra, ^1H NMR spectra, fluorescence studies and UV-vis spectra. The likely structure of the rare earth complexes is [Ln L_2•$(NO_3)_2$]•NO_3 [Ln(III) = La, Sm, Nd and Tb; L is the ligand 3-carbaldehyde chromone-(benzoyl) hydrazone].

DNA binding studies

Electronic absorption spectroscopy

Before reacting the ligand and its rare earth complexes interacting with CT DNA, their solution behavior in buffer solution at room temperature was monitored by UV-vis spectroscopy for 24 h. Liberation of the ligand and its complexes was not observed under these conditions. These suggest that the ligand and its complexes are stable under the conditions studied.

Table 1 Fluorescecne spectra and fluorescecne quantum yields $\varnothing_f$ of the ligand and Sm(III) complex in different solutions at room temperature. All the emission and excitation slit widths were 3 nm

Compound	Solvent	λ_{ex} (nm)	λ_{em} (nm)	Emission intensity	$\varnothing_f$
L	Ethanol	395	489	41.344	0.1213
	Methanol	405	489	9.739	0.1254
	DMF	374	431	30.337	0.2356
	CH_3CN	396	503	0.793	0.0869
	THF	371	498	1.203	0.0754
Sm(III) complex	Ethanol	409	497	16.746	0.0223
	Methanol	405	496	10.625	0.0154
	DMF	374	432	24.158	0.0312
	CH_3CN	357	489	1.757	0.0112
	THF	361	452	3.022	0.0123

The binding abilities of the ligand and rare earth complexes with CT DNA can be characterized by measuring their effects on the UV-vis spectroscopy. Complexes binding to DNA via an intercalation mode usually results in hypochromism and bathochromism due to intercalative mode involving a strong stacking interaction between an aromatic chromophore and the base pairs of DNA [40]. In the present investigation, the interaction of complexes with DNA has been studied. The binding of complexes to DNA led to decrease in the absorption intensities with a small amount of red shifts in the UV-vis absorption spectra. After intercalating the base pairs of DNA, the π^* orbital of the intercalated ligand can couple with the π orbital of the DNA base pairs, thus, decreasing the $\pi \rightarrow \pi^*$ transition energy and resulting in the bathochromism. On the other hand, the coupling π orbial is partially filled by electrons, thus, decreasing the transition probalities and concomitantly resuting in the hypochromism [41]. Therefore, in order to obtain evidence for the possibility of binding mode of each compound to CT DNA, spectroscopic titration of a solution of compounds with CT DNA should be performed.

The electronic absorption spectra of the free ligand and its complexes in the absence and presence of CT DNA are given in Fig. 3. As shown, in the presence of DNA, the absorption bands of the ligand, La(III), Sm(III), Nd(III) and Tb(III) complexes at about 308 nm exhibited hypochromism of about 34.5%, 44.2%, 35.2%, 51.0% and 36.9%, respectively. The hypochromism observed for the rare earth complexes are all accompanied by a small red shift by about 3 nm. All these results suggest that the complexes can interact with CT DNA quite probably by intercalating the compounds into DNA base pairs, so we can conclude that the free ligand and its metal complexes can interact with CT DNA via a same mode (intercalation).

EB (a typical indicator of intercalation) quenching assay was performed to further test the binding modes of DNA to these investigated compounds [42]. Figure 4 shows the electronic absorption spectra when EB was employed. The absorbance of the buffer solution is highest when there is EB alone. After adding CT DNA into the buffer solution, the absorbance decreases. However, it increases when the ligand and metal complexes were added dropwise into the buffer solution. In addition, the maximal absorption of EB at 479 nm decreases and shiftes to 494 nm in the presence of CT DNA, which is characteristic of intercalation mode. Curve (B) in Fig. 4 shows the absorption of a mixture solution of EB, DNA and Sm(III) complex. It is also found that the absorption at 494 nm has increased comparing with curve (C). These may result from two reasons: (1) EB bound to the free ligand and metal complexes strongly,

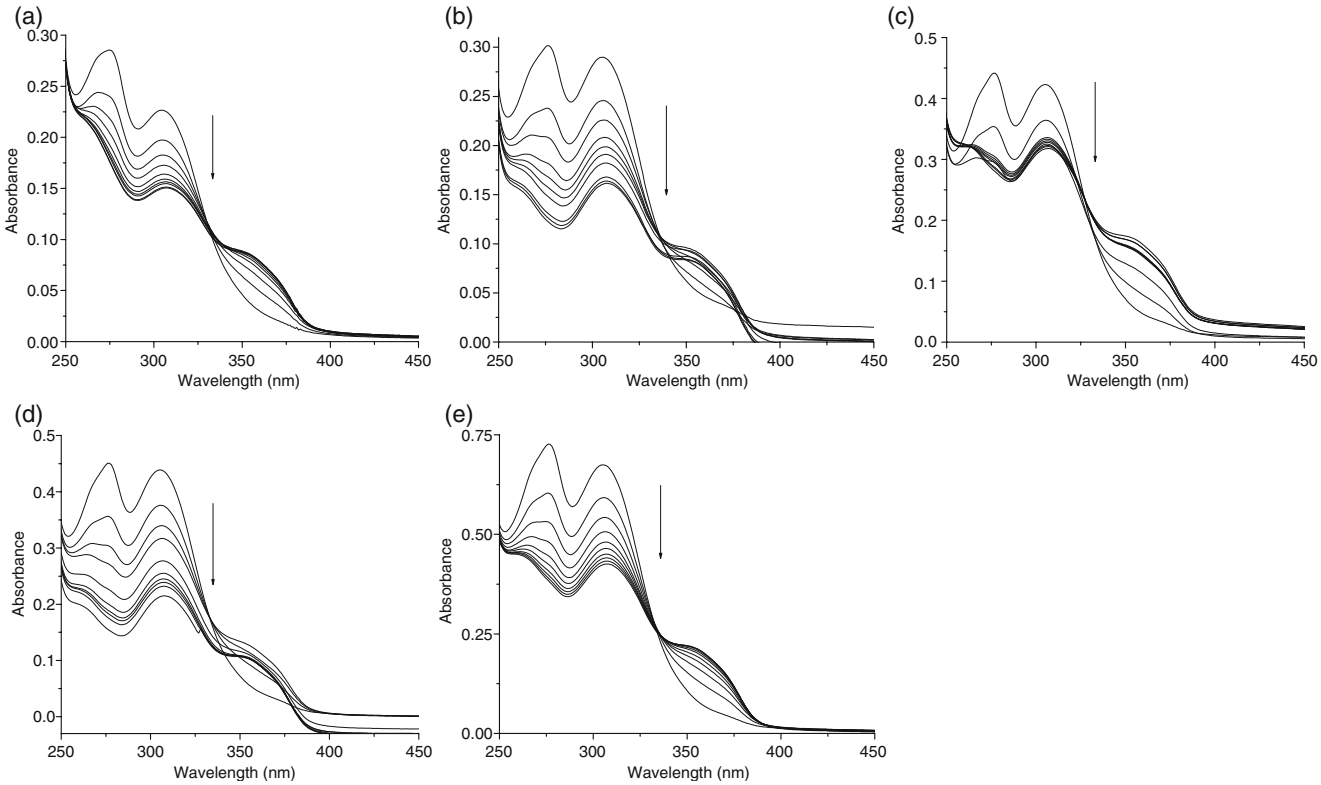

Fig. 3 Electronic absorption spectra of the ligand **a**, La(III) **b**, Sm(III) **c**, Nd(III) **d** and Tb(III) **e** complexes (10 μM) in the absence (top spectrum) and presence of increasing amounts of CT DNA (2.5, 5.0, 7.5, 10.0, 12.5, 15.0, 17.5, 20.0 and 22.5 μM; subsequent spectra). Arrow shows the absorbance changes upon increasing DNA concentration

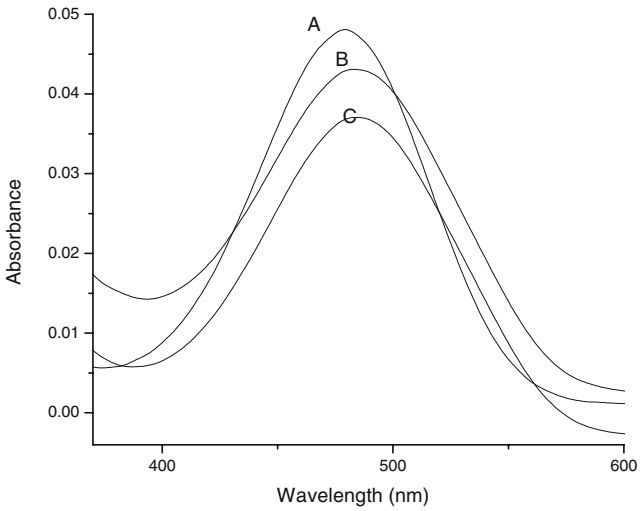

Fig. 4 The ultraviolet visible absorption spectra of 1×10^{-5} M EB (A); (A)+2.5×10^{-5} M DNA (C); (C)+2.5×10^{-5} M Sm(III) complex in Tris-HCl buffer (5 mM Tris–HCl, 50 mM NaCl, pH 7.1) solution

resulting in the decrease of the amount of EB intercalated into DNA; (2) there exists competitive intercalation between the free ligand and metal complexes and EB with DNA, so releasing some free EB from DNA–EB system. However, the former reason could be precluded because there were no new absorption peaks appearing. Thus, we can come to a conclusion that Sm(III) complex can displace EB from its DNA-EB system. Quite similar results are also observed for other rare earth complexes.

Fluorescence spectra

The steady-state emission spectra of 10 μM solutions of the rare earth complexes in Tris-HCl buffer show an increase in the emission intensity with successive addition of CT DNA at room temperature (Fig. 5). According to the Scatchard equation, a plot of r/C_f versus r gave K_b values of $(7.39\pm0.48)\times10^5$, $(2.02\pm0.91)\times10^6$, $(1.42\pm0.74)\times10^6$, $(7.39\pm0.48)\times10^6$, $(1.21\pm0.60)\times10^6$ M^{-1} from the fluorescence data for the ligand, La(III), Sm(III), Nd(III) and Tb(III) complexes, respectively. Results obtained from fluorescence spectra suggest that all the compounds are protected from solvent water molecules by the hydrophobic environment inside the DNA helix and that the metal complexes can be protected more efficiently than the free ligand alone. This implies that all the metal complexes and free ligand can insert between DNA base pairs deeply and the metal complexes can bind to DNA more strongly than the free ligand alone. Since the hydrophobic environment inside the DNA helix reduces the accessibility of solvent water molecules to the compound and the compound mobility is restricted at the certain binding site, a decrease of the vibrational modes of relaxation results. The binding of the compounds to DNA leading to a significantly increase in emission intensity also agrees with those observed for other intercalators [43]. The fluorescence spectra show that the rare earth complexes can bind to DNA more strongly and deeply than the free ligand alone, The higher binding affinities of the complexes are probably attributed to the extension of the π system of the intercalated ligand due to the coordination of rare earth ions, which also leads to a planar area greater than that of the free ligand and the coordinated ligand penetrating more deeply into and stacking more strongly with the base pairs of DNA.

EB is one of the most sensitive fluorescence probes that can bind to DNA and the fluorescence of EB increases after intercalating into DNA base pairs [44]. If the complexes intercalate into the DNA base pairs, leading to a decrease in the binding sites of DNA available for EB and resulting in the decrease in the fluorescence intensity of the DNA-EB system. The reduction of the fluorescence emission intensity gives a criteria to investigate the DNA binding propensity of the complexes and the stacking interaction (intercalation) between the adjacent DNA base pairs [45]. Figure 6 shows the emission spectra of the DNA–EB system with increasing amounts of the rare earth complexes and free ligand. The addition of the compounds to the DNA-bound EB solutions caused obvious reduction in emission intensities and the quenching of EB bound to DNA by the rare earth complexes is in good agreement with the linear Stern-Volmer equation. In the plots of F_0/F versus [Q], K_q is given by the ratio of the slope to the intercept and K_q values for the ligand, La(III), Sm(III), Nd(III) and Tb(III) complexes are $(1.39\pm0.01)\times10^4$ M^{-1}, $(5.66\pm0.07)\times10^4$ M^{-1}, $(5.16\pm0.04)\times10^4$ M^{-1}, $(2.42\pm0.05)\times10^4$ M^{-1} and $(4.62\pm0.04)\times10^4$ M^{-1}. The results show that all the compounds can bind to DNA and the complexes bind to DNA more strongly than the free ligand, which also validate the electronic absorption spectral results. Since these changes indicate only one kind of quenching process, it may be concluded that the complexes and free ligand can bind to DNA via the same mode (intercalation).

In the aqueous solution, iodide and ferrocyanide anions quench the fluorescence of complexes very efficiently, and we used potassium iodide as the quencher to determine the relative accessibilities of the free and bound Sm(III) complex. Emission spectra for the Sm(III) complex and potassium iodide with absence and presence of CT DNA are illustrated in the titration curves (Fig. 7). Compared to the emission spectra of Sm(III) complex in Tris-HCl buffer solution alone, fluorescence intensities decrease with the addition of potassium iodide regardless whether the buffer solution contains CT DNA and the quenching plots illustrated that the quenching studies of the Sm(III) complex are in good agreement with the linear Stern–Volmer equation and the slopes were calculated by the

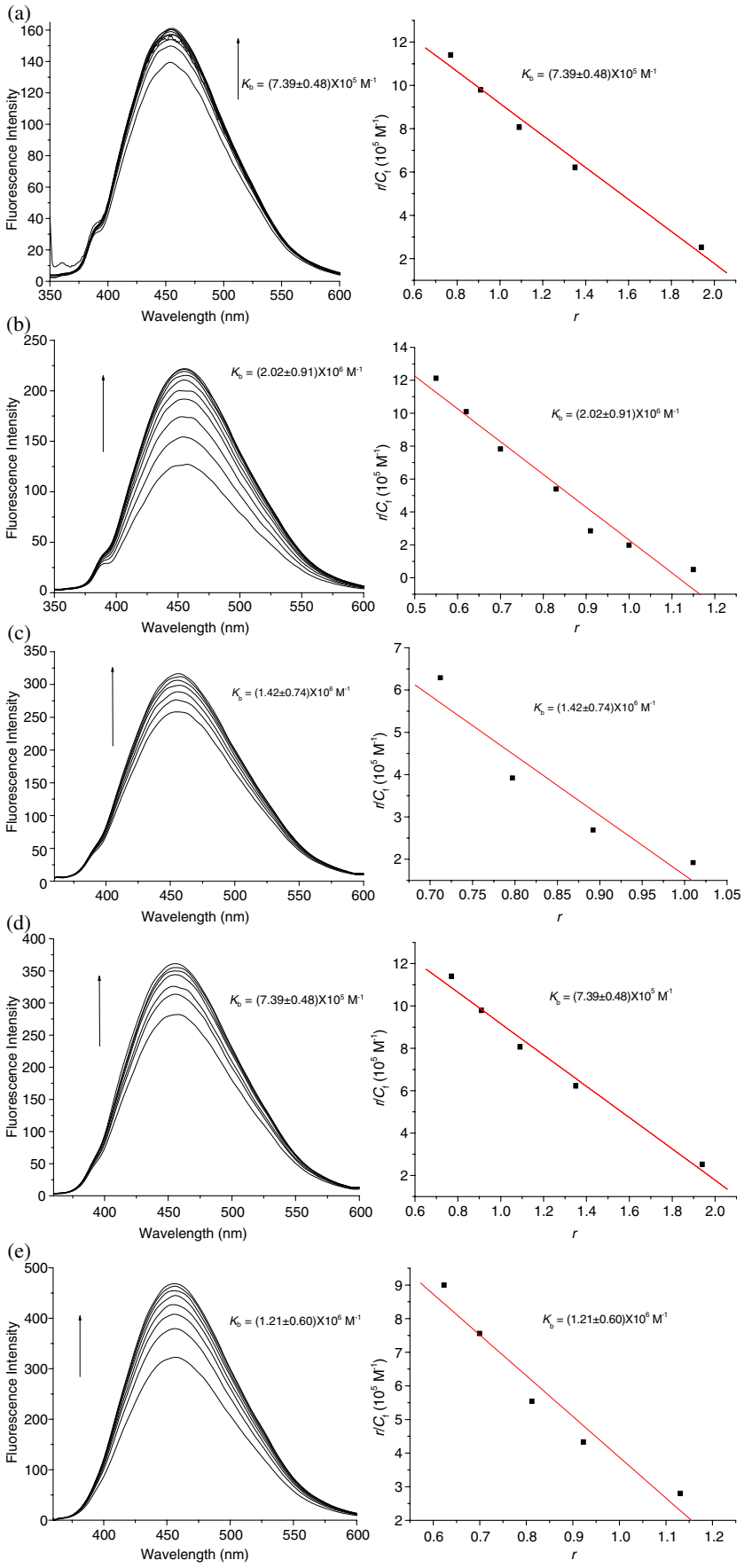

Fig. 5 The emission enhancement spectra of the free ligand **a** (λ_{ex}=451 nm, λ_{em}=342 nm), La (III) **b** (λ_{ex}=454 nm, λ_{em}=342 nm), Sm(III) **c** (λ_{ex}=455 nm, λ_{em}=347 nm), Nd(III) **d** (λ_{ex}=456 nm, λ_{em}=345 nm) and Tb (III) **e** (λ_{ex}=457 nm, λ_{em}=347 nm) complexes (10 μM) in the absence (bottom spectrum) and presence of increasing amounts of CT DNA (2.5, 5.0, 7.5, 10.0, 12.5 and 15.0 μM; subsequent spectra). Arrows show the emission intensity changes upon increasing DNA concentration. *Inset:* Scatchard plot of the fluorescence titration data of ligand and rare earth complexes, K_b (a)=(7.39±0.48)×10^5; K_b (b)=(2.02±0.91)×10^6 M^{-1}; K_b (c)=(1.42±0.74)×10^6 M^{-1}; K_b (d)=(7.39±0.48)×10^6 M^{-1}; K_b (e)=(1.21±0.60)×10^6 M^{-1}

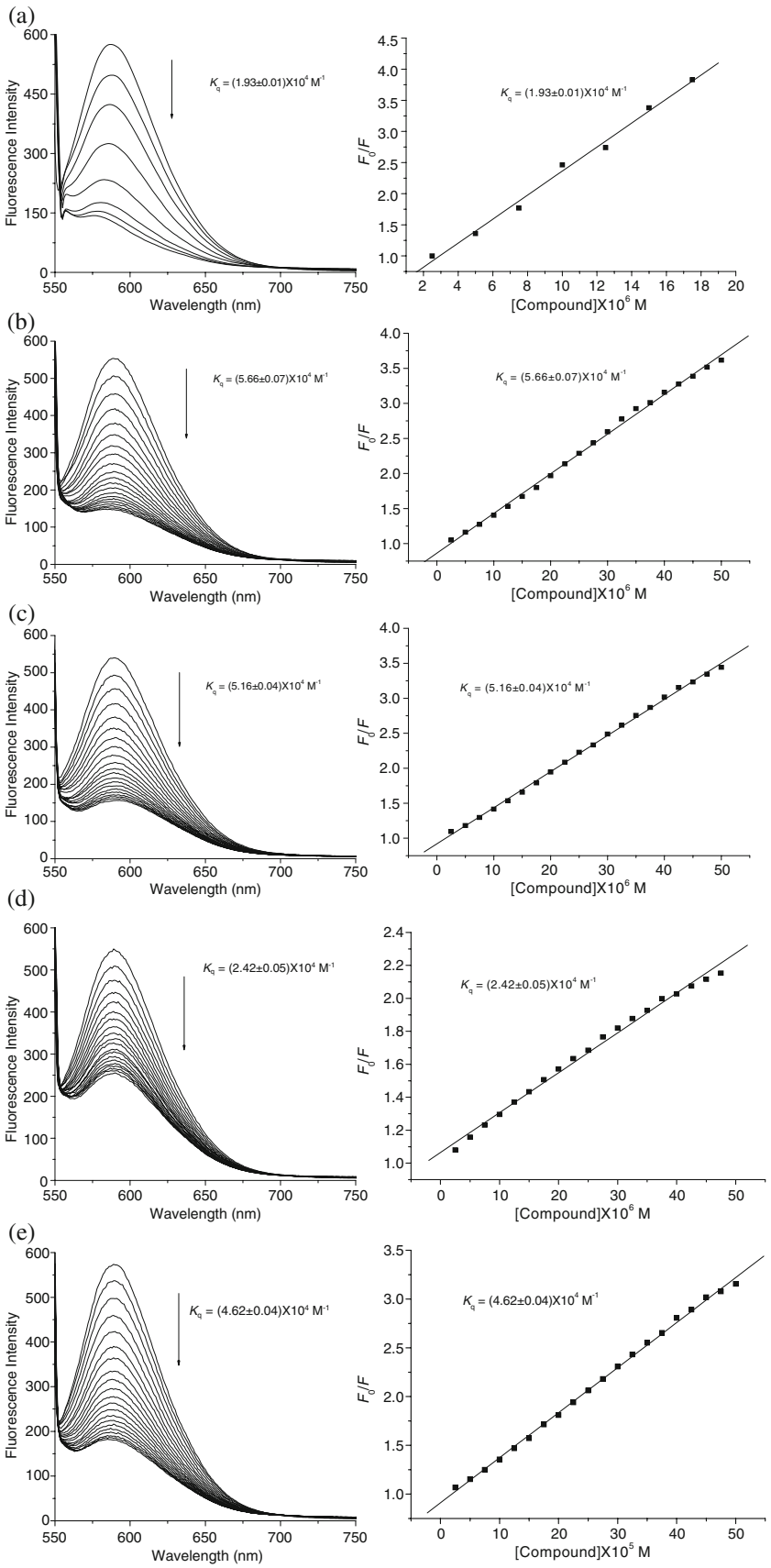

Fig. 6 The emission spectra of DNA-EB system λ_{ex}=525 nm, λ_{em}=550-650 nm, in the presence of 0, 25.0, 50.0, 75.0, 100.0, 125.0, 150.0 and 175.0 μM free ligand **a** and 0, 2.5, 5, 7.5, 10, 12.5, 15, 17.5, 20.0, 22.5, 25, 27.5, 30.0, 32.5, 35.0, 37.5, 40, 42.5, 45, 47.5 and 50.0 μM La(III) **b**, Sm(III) **c**, Nd(III) **d** and Tb(III) **e** complexes. Arrows show the emission intensity changes upon increasing ligand. *Inset:* Stern Volmer plot of the fluorescence titration data of ligand and complexes, K_q (a)=(1.39±0.01)×10^4 M^{-1}; K_q (b)=(5.66±0.07)×10^4 M^{-1}; K_q (c)=(5.16±0.04)×10^4 M^{-1}; K_q (d)=(2.42±0.05)×10^4 M^{-1}; K_q (e)=(4.62±0.04)×10^4 M^{-1}

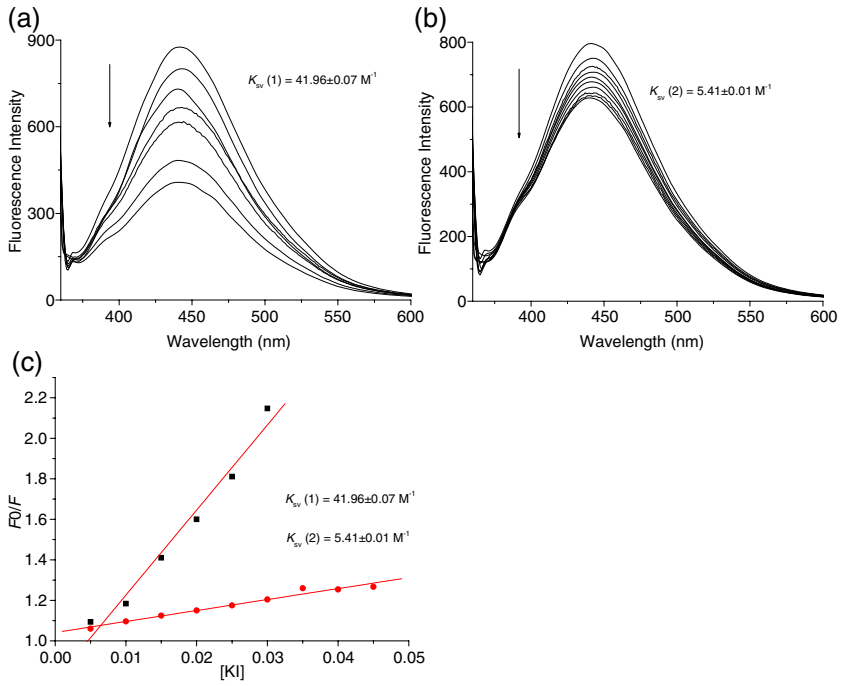

Fig. 7 **a** Fluorescence spectra of Sm(III) complex (10 μM) (λ_{ex}=446 nm, λ_{em}=674 nm) with increasing concentration of KI (5, 10, 15, 20, 25, 30 and 35 mM). **b** Fluorescence spectra of Sm(III) complex (10 μM) (λ_{ex}=442 nm, λ_{em}=664 nm) and DNA (20 μM) system with increasing concentration of KI (5, 10, 15, 20, 25, 30 and 35 mM). **c** *Inset*: Stern Volmer plot of the fluorescence titration data of Sm(III) complex. Effect of KI concentration (1: Sm(III) complex + KI; 2: Sm(III) complex + KI + CT DNA). K_{sv} (1)= 41.96±0.07 M^{-1}, K_{sv} (2)=5.41± 0.01 M^{-1}

linear least-squares method. The observed quenching constants (K_{sv}) were 5.41±0.01 and 41.96±0.07 M^{-1} with and without CT DNA, respectively. The quenching of the Sm(III) complex fluorescence was in fact enhanced by a factor of about 8 when the Sm(III) complex was bound to the DNA helix. The values of K_{sv} were used to deduce the interaction mode of the fluorescence probe with DNA. Higher binding constants should correspond to the better protection by the DNA and a stronger inhibition of quenching by anionic species. Similar results can be obtained for other complexes and then we can conclude that the metal complexes are intercalated into the DNA helix and they should be protected from the anionic quencher, owning to the base pairs above and below the intercalators [46].

The effect of the ionic strength on the complexes fluorescence intensity was tested by the addition of a strong electrolyte, such as NaCl, instead of potassium iodide. Cations of the salts can neutralize the negatively charged phosphate. If the compound binds to DNA through an electrostatic interaction mode, the surface of DNA will be surrounded by the sodium ions with the increase of ionic strength. Then the compound has difficulty to approach DNA molecules and the strength of compounds binding to DNA decreases, then the degrees of fluorescence quenching also decreases [21]. As seen from Fig. 8, addition of NaCl

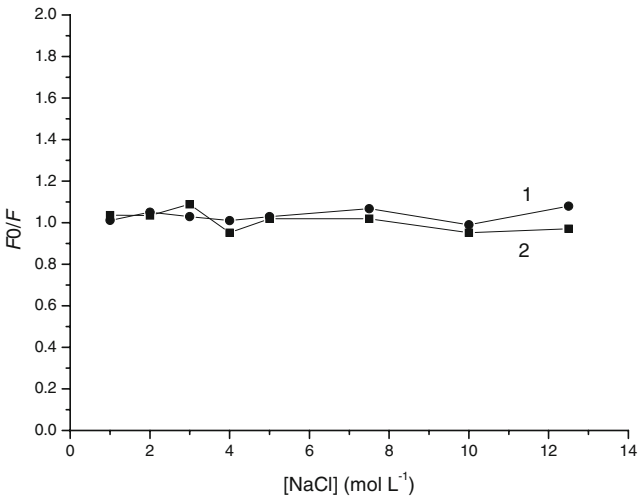

Fig. 8 Effect of NaCl concentration (1: Sm(III) complex + NaCl; 2: Sm(III) complex + NaCl + CT DNA)

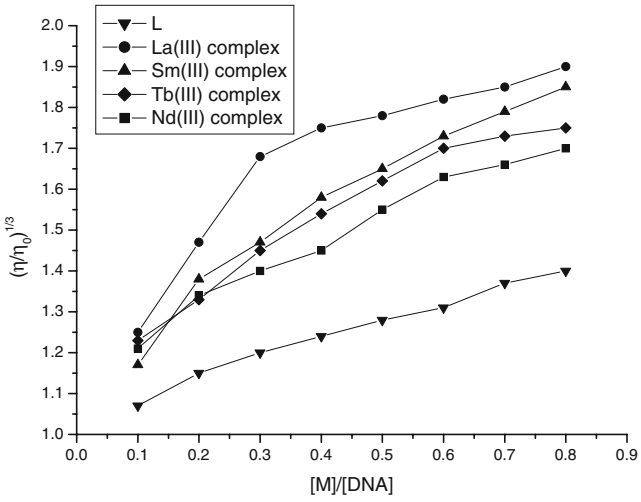

Fig. 9 Effects of increasing amounts of the ligand and its rare earth complexes on the relative viscosity of CT DNA at 25.0±0.1 °C

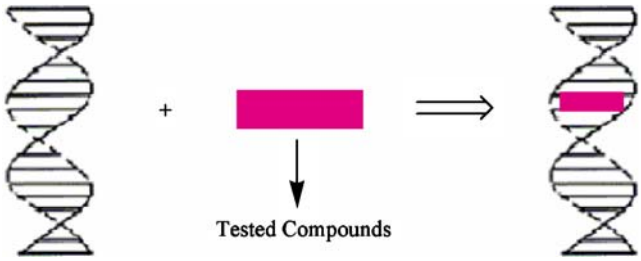

Fig. 10 Molecular mode for the rare earth complexes (via an intercalative mode)

to the Sm(III) complex in the absence and presence of CT DNA had little or no effects on the fluorescence intensity, showing that the interaction of the Sm(III) complex with CT DNA is not through an electrostatic interaction. Similar results also can be gained for other complexes. Hereby, we can conclude that the compounds interact with DNA is not via an electrostatic mode.

Viscosity measurements

Hydrodynamic measurements sensitive to length changes, as reflected in viscosity and sedimentation, are regarded as the least ambiguous and the most critical tests of a binding model in solution in the absence of crystallographic structural data [47]. A classical intercalation model demands that the DNA helix must lengthen as base pairs are separated to accommodate the binding complexes, leading to the increase of DNA viscosity, as for the behaviors of the known DNA intercalators [48]. In contrast, a partial and/or non-classical intercalation of the complex could bend (or kink) the DNA helix, reducing its viscosity concomitantly [47]. In addition, some compounds such as $[Ru(bpy)_3]^{2+}$, which interacts with DNA by an electrostatic binding mode, have no influence on DNA viscosity [49]. To further elucidate the binding mode of the present complexes, viscosity measurements were carried out by keeping [DNA]=5 μM and varying the concentration of the compounds.

The changes in relative viscosity of CT DNA in the presence of the ligand and complexes are shown in Fig. 9. As seen from Fig. 9, upon increasing amounts of the ligand and complexes, the relative viscosities of DNA increase steadily with increasing concentrations of ligand and complexes. The increased degree of viscosity, which may depend on the binding affinity of compounds to DNA, following the order of La(III) complex >Sm(III) complex >Tb(III) complex >Nd(III) complex >L. These results suggest that all the title complexes and ligand intercalate between the DNA base pairs and the binding affinities of the complexes are higher than that of the free ligand, which is consistent with the above experimental results.

On the basis of all the spectroscopic studies together with the viscosity measurements, we find that the rare earth complexes and free ligand can bind to CT DNA via an intercalative mode (Fig. 10) and the complexes bind to CT DNA more strongly and deeply than the free ligand alone.

Antioxidant activity

Since the synthesized ligand and its rare earth complexes exhibit good DNA binding affinity, it is considered worthwhile to investigate their other biological activities, such as antioxidant activity. The antioxidant activity of chromones and their derivatives has attracted increasing interests and been extensively investigated, mainly in the vitro system [50]. It has been reported that over production of free radicals may induce some oxidative damages to

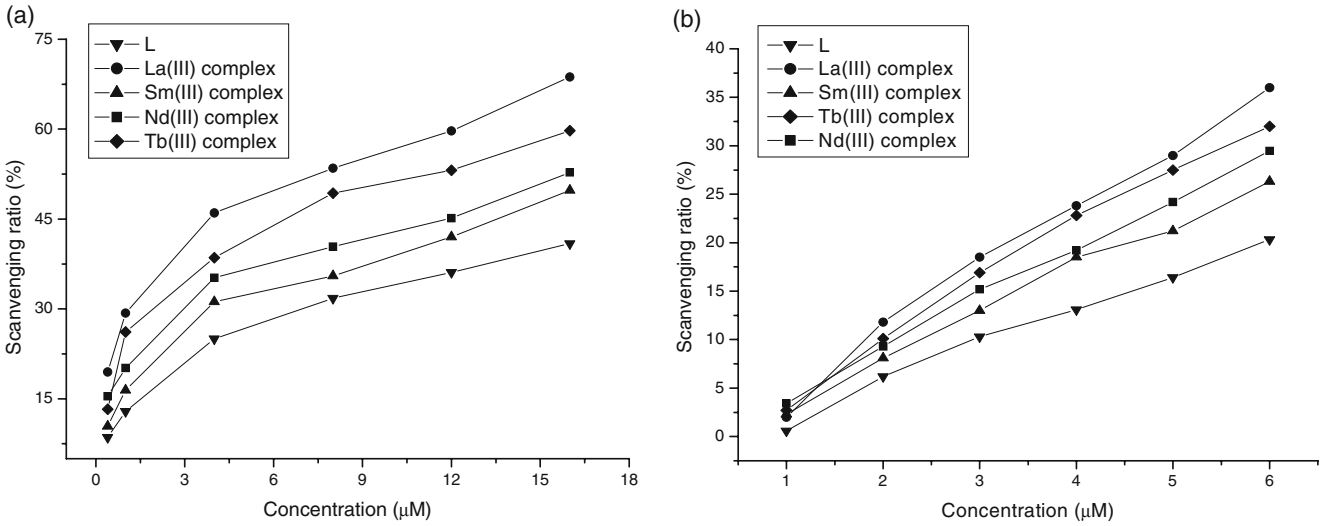

Fig. 11 Scavenging effect of the ligand and its rare earth complexes on $O_2^{\bullet-}$ **a** and $HO^{\bullet}$ **b**

biomolecules such as carbohydrates, proteins, lipids and DNA, thus accelerating aging, cancer, cardiovascular diseases, inflammation and so on [51]. So, in this paper, the ligand and its rare earth complexes were studied to investigate their antiradicals ability by comparing their scavenging effects on hydroxyl radical ($HO^{\bullet}$) and superoxide radical ($O_2^{\bullet-}$).

Figure 11a shows the plots of superoxide radical scavenging effect (%) for the ligand and complexes. We find that the inhibitory effect of the compounds tested on $O_2^{\bullet-}$ is concentration dependent and the suppression ratio increases with increasing sample concentrations in the range tested. The average suppression ratio of the free ligand (IC_{50}= 58.48 μM) for $O_2^{\bullet-}$ is the least in all compounds. The La(III) complex (IC_{50}=5.00 μM) is the most effective one in the rare earth complexes, which may be induced by the metal ions.

Figure 11b shows the plots of hydroxyl radical scavenging effect (%) for the ligand and complexes. The inhibitory effect of the compounds is marked and the average suppression ratio for $HO^{\bullet}$ increases with the increaseing compound concentration. The order of the suppression ratio of the tested compounds for HO is La(III) complex >Tb(III) complex >Nd(III) complex >Sm(III) complex >L. The average suppression ratio of the rare earth complexes is better than the free ligand alone. It is clearly shown that metal complexes exhibit considerable scavenging abilities due to the chelation of organic molecules to rare earth ions and the rare earth ions such as La(III), Tb(III), Nd(III), Sm (III) exert differential and selective effects on scavenging radicals of the biological system. In order to prepare more effective and lower poisonous antioxidants, the metal complexes we studied in this paper deserve to be further researched.

Conclusions

In summary, a new ligand, 3-carbaldehyde chromone-(benzoyl) hydrazone, and its four rare earth complexes have been prepared and characterized. The Sm(III) complex is red-fluorescent in the solid state and its emission intensity are highly solvent-dependent. In addition, their DNA binding properties and antioxidant activities were studied systematically. Experimental results indicate that the ligand and its complexes can bind to DNA via an intercalation mode and the complexes have better DNA binding affinity than the free ligand alone. Furthermore, the complexes have more active scavenging effects on $O_2^{\bullet-}$ and $HO^{\bullet}$. Our work clearly indicates that rare earth-based complexes have many potential practical applications, such as understanding the mechanisms of interaction between compounds and DNA, the development of potential acid molecular probes and new therapeutic reagents for diseases.

Acknowledgements This work is supported by the National Natural Science Foundation of China (20475023) and Gansu NSF (0710RJZA012).

References

1. Kelland LR (2005) Overcoming the immortality of tumour cells by telomere and telomerase based cancer therapeutics-current status and future prospects. Eur J Cancer 41(7):971–979
2. Uma V, Kanthimath M, Weyhermuller T, Nair BU (2005) Oxidative DNA cleavage mediated by a new copper (II) terpyridine complex: crystal structure and DNA binding studies. JInorgChem 99(12):2299–2307
3. Erkkila KE, Odom DT, Barton JK (1999) Recognition and reaction of metallointercalators with DNA. Chem Rev 99(9):2777–2795
4. Arockiasamy DL, Radhika S, Parthasarathi R, Nair BU (2009) Synthesis and DNA-binding studies of two ruthenium(II) complexes of an intercalating ligand. Eur J MedChem 44(5):2044–2051
5. Wang BD, Yang ZY, Crewdson P, Wang DQ (2007) Synthesis, crystal structure and DNA-binding studies of the Ln(III) complex with 6-hydroxychromone-3-carbaldehyde benzoyl hydrazone. J Inorg Biochem 101(10):1492–1504
6. Kumar CV, Barton JK, Turro NJ (1985) Photophysics of ruthenium complexes bound to double helical DNA. J Am Chem Soc 107(19):5518–5523
7. Xu H, Zheng KC, Chen Y, Li YZ, Lin LJ, Li H, Zhang PX, Ji LN (2003) Effects of ligand planarity on the interaction of polypyridyl Ru(II) complexes with DNA. Dalton Trans 3(11):2260–2268
8. Mahadvan S, Palaniandavar M (1997) Spectroscopic and voltammetric studies of copper(II) complexes of bis(pyrid-2-yl)-di/trithia ligands bound to calf thymus DNA. Inorg Chim Acta 254(2):291–302
9. Xu H, Zheng KC, Deng H, Lin LJ, Zhang QL, Ji LN (2003) Effects of the ancillary ligands of polypyridyl ruthenium(III) complexes on the DNA-binding behaviors. New J Chem 27 (8):1255–1263
10. Asadi M, Safaei E, Ranjbar B, Hasani L (2004) Thermodynamic and spectroscopic study on the binding of cationic Zn(II) and Co(II) tetrapyridinoporphyrazines to calf thymus DNA: the role of the central metal in binding parameters. New J Chem 28(10):1227–1234
11. Bisi CC, Carugo O (1989) Studies on fluorescent lanthanide complexes. New complexes of lanthanides(III) with coumarinic-3-carboxylic acid. Inorg Chim Acta 159(2):157–161
12. Ci YX, Li YZ, Chang WB (1991) Fluorescence reaction of terbium(III) with nucleic acids in the presence of phenanthroline. Anal Chim Acta 248(2):589–594
13. Horne DA, Dervan PB (1990) Recognition of mixed-sequence duplex DNA by alternate-strand triple-helix formation. J Am Chem Soc 112(6):2435–2437
14. Moser HE, Dervan PB (1987) Sequence-specific cleavage of double helical DNA by triple helix formation. Science 238(4827):645–650
15. Sosnovskikh VY (2003) Synthesis and reactions of halogen-containing chromones. Russ Chem Rev 72(6):489–516
16. Athanasellis G, Melagraki G, Afantitis A, Makridima K, Markopoulou OI (2006) A simple synthesis of functionalized 2-amino-3-cyano-4-chromones by application of the N-hydroxybenzotriazole methodology. Arkivoc 10:28–34
17. Singh G, Singh R, Girdhar NK, Ishar MPS (2002) A versatile route to 2-alkyl-/aryl-amino-3-formyl- and hetero-annelated-chromones, through a facile nucleophilic substitution at C2 in 2-(N-methylanilino)-3-formylchromones. Tetrahedron 58(12):2471–2480
18. Piao LZ, Park HR, Park YK, Lee SK, Park JH, Park MK (2002) Mushroom tyrosinase inhibition activity of some chromones. Chem Pharm Bull 50(3):309–311

19. Cai YZ, Luo Q, Sun M, Corke H (2004) Antioxidant activity and phenolic compounds of 112 traditional Chinese medicinal plants associated with anticancer. Life Sci 74(17):2157–2184
20. Heim KE, Tagliaferro AR, Bobilya DJ (2002) Flavonoid antioxidants: chemistry, metabolism and structure-activity relationships. J Nutr Biochem 13(10):572–584
21. Howe GM, Wu KC, Bauer WR, Lippard SJ (1976) Binding of platinum and palladium metallointercalation reagents and antitumor drugs to closed and open DNAs. Biochem 15(19):4339–4346
22. Eftink MR, Ghiron CA (1981) Fluorescence quenching studies with proteins. Anal Biochem 114(2):199–227
23. Kumar CV, Turner RS, Asuncion EH (1993) Groove binding of a styrylcyanine dye to the DNA double helix: the salt effect. J Photochem Photobiol A: Chem 74(2–3):231–238
24. Eriksson M, Leijon M, Hiort C, Norden B, Graeslund A (1994) Binding of Δ- and Δ-$[Ru(phen)_3]^{2+}$ to $[d(CGCGATCGCG)]_2$ studied by NMR. Biochem 33(17):5031–5040
25. Xiong Y, He XF, Zou XH, Wu JZ, Chen XM, Ji LN, Li RH, Zhou JY, Yu KB (1999) Interaction of polypyridyl ruthenium(II) complexes containing non-planar ligands with DNA. J Chem Soc, Dalton Trans: Inorg Chem 1:19–24
26. Winterbourn CC (1979) Comparison of superoxide with other reducing agents in the biological production of hydroxyl radicals. Biochem J 182(2):625–628
27. Winterbourn CC (1981) Hydroxyl radical production in body fluids. Roles of metal ions, ascorbate and superoxide. Biochem J 198(1):125–131
28. Nohara A, Umetani T, Sanno Y (1973) Facile synthesis of chromone-3-carboxaldehyde, chromone-3-carboxylic acid, and 3-hydroxymethylchromone. Tetrahedron Lett 14(22):1995–1998
29. Geary WJ (1971) Use of conductivity measurements in organic solvents for the characterization of coordination compounds. Coord Chem Rev 7(1):81–122
30. Marchetti F, Pettinari C, Pettinari R, Cingolani A, Leonesi D, Lorenzotti A (1999) Group 12 metal complexes of tetradentate N_2O_2-Schiff-base ligands incorporating pyrazole: synthesis, characterisation and reactivity toward S-donors, N-donors, copper and tin acceptors. Polyhedron 18(23):3041–3050
31. Narang KK, Singh VP (1993) Synthesis and characterization of cobalt(II), nickel(II), copper(II) and zinc(II) complexes with acetylacetone bis-benzoylhydrazone and acetylacetone bis-isonicotinoylhydrazone. Transition Met Chem 18(3):287–290
32. Wang BD, Yang ZY, Zhang DW, Wang Y (2006) Synthesis, structure, infrared and fluorescence spectra of new rare earth complexes with 6-hydroxy chromone-3-carbaldehyde benzoyl hydrazone. Spectrochim acta Part A 63(1):213–219
33. Lehn JM (1990) Perspectives in supramolecular chemistry: from molecular recognition to molecular information processing and self organization. Angew Chem Int Ed Engl 29(11):1304–1319
34. Latva M, Takalo H, Simberg K, Ankare KJ (1995) Enhanced Eu^{III} ion luminescence and efficient energy transfer between lanthanide chelates within the polymeric structure in aqueous solutions. J Chem Soc, Perkin Trans 2(5):995–999
35. Wu SL, Wu YL, Yang YS (1992) Rare earth(iii) complexes with indole-derived acetylacetones II. luminescent intensity for europium (iii) and terbium(iii) complexes. J Alloys Compd 180(2):399–402
36. Sato S, Wada M (1970) Relations between intramolecular energy transfer efficiencies and triplet state energies in rare Earth β-diketone chelates. Bull Chem Soc Jpn 43(7):1955–1962
37. Wua WN, Tang N, Yan L (2008) Rare earth complexes with a novel ligand N-(naphthalen-2-yl)-N-phenyl-2-(quinolin-8-yloxy) acetamide: preparation and spectroscopic studies. Spectrochim Acta Part A 71(4):1461–1465
38. Tang Y, Tang KZ, Liu WS, Tan MY (2008) Assembly, crystal structure, and luminescent properties of three-dimensional (10,3)-a netted rare earth coordination polymers. Sci China, Ser B 51 (7):614–622
39. Latva M, Takalo H, Mukkala VM, Matachescu C, Rodríguez-Ubis JC, Kankare J (1997) Correlation between the lowest triplet state energy level of the ligand and lanthanide(III) luminescence quantum yield. J Lumin 75(2):149–169
40. Gao F, Chao H, Zhou F, Yuan YX, Peng B, Ji LN (2006) DNA interactions of a functionalized ruthenium(II) mixed-polypyridyl complex [Ru(bpy)2 ppd]2+. J Inorg Biochem 100(9):1487–1494
41. Pyle AM, Rehmann JP, Meshoyrer R, Kumar CV, Turro NJ, Barton JK (1989) Mixed-ligand complexes of ruthenium(II): factors governing binding to DNA. J Am Chem Soc 111(8):3051–3058
42. Wilson WD, Ratmeyer L, Zhao M, Strekowski L, Boykin D (1993) The search for structure-specific nucleic acid-interactive drugs: effects of compound structure on RNA versus DNA interaction strength. Biochem 32(15):4098–4104
43. Xu H, Zheng KC, Lin LJ, Li H, Gao Y, Ji LN (2004) Effects of the substitution positions of Br group in intercalative ligand on the DNA-binding behaviors of Ru(II) polypyridyl complexes. J Inorg Biochem 98(1):87–97
44. Le-Pecq JB, Paoletti C (1967) A fluorescent complex between ethidium bromide and nucleic acids. J Mol Biol 27(1):87–106
45. Lee M, Rhodes AL, Wyatt MD, Forrow S, Hartley JA (1993) GC base sequence recognition by oligo(imidazolecarboxamide) and C-terminus-modified analogues of distamycin deduced from circular dichroism, proton nuclear magnetic resonance, and methidiumpropylethylenediaminetetraacetate-iron(II) footprinting studies. Biochem 32(16):4237–4245
46. Lerman LS (1961) Structural considerations in the interaction of deoxyribonucleic acid and acridines. J Mol Biol 3:18–30
47. Satyanarayana S, Dabrowiak JC, Chaires JB (1993) Tris(phenanthroline)ruthenium(II) enantiomer interactions with DNA: mode and specificity of binding. Biochem 32(10):2573–2584
48. Liu JG, Zhang QL, Shi XF, Ji LN (2001) Interaction of $[Ru(dmp)_2(dppz)]^{2+}$ and $[Ru(dmb)_2(dppz)]^{2+}$ with DNA: effects of the ancillary ligands on the DNA-binding behaviors. Inorg Chem 40(19):5045–5050
49. Liu JG, Ye BH, Li H, Zhen QX, Ji LN, Fu YH (1999) Polypyridyl ruthenium(II) complexes containing intramolecular hydrogen-bond ligand: syntheses, characterization, and DNA-binding properties. J Inorg Biochem 76(3–4):265–271
50. Wang Q, Yang ZY, Qi GF, Qin DD (2009) Synthesis, crystal structure, antioxidant activities and DNA-binding studies of the Ln(III) complexes with 7-methoxychromone-3-carbaldehyde-(4'-hydroxy) benzoyl hydrazone. Eur J Med Chem 44(6):2425–2433
51. Proctor PH, Reynolds ES (1984) Free radicals and disease in man. Physiol Chem Phys Med NMR 16(3):175–195